Isothermal Crystallization Behavior of Hybrid Biocomposite Consisting of Regenerated Cellulose Fiber, Clay, and Poly(lactic acid)

Seung-Hwan Lee,[1,2] Siqun Wang,[1] Yoshikuni Teramoto[2]

[1]*Forest Product Center, Forestry, Wildlife and Fisheries, University of Tennessee, Knoxville, Tennessee*
[2]*National Institute of Advanced Industrial Science and Technology (AIST), Biomass Technology Research Center (BTRC), 2-2-2, Hiro-Suehiro, Kure, Hiroshima 737-0197, Japan*

Received 10 February 2006; accepted 29 December 2006
DOI 10.1002/app.26853
Published online 18 January 2008 in Wiley InterScience (www.interscience.wiley.com).

ABSTRACT: Quantitative analysis of isothermal crystallization kinetics of PLA/clay nanocomposite and PLA/clay/regenerated cellulose fiber (RCF) hybrid composite has been conducted. The crystallization rate constant (k) according to Avrami equation was higher in PLA/clay nanocomposite than in PLA/clay/RCF hybrid composite at the same crystallization temperature. The equilibrium melting temperature obtained by Hoffman–Weeks equation was almost same in both composites, whereas stability parameter was greater in hybrid composite than in nanocomposite. Activation energy of hybrid composite for crystallization was larger than that of nanocomposite. The value of nucleation parameter (K_g) and surface free energy (s_e) of hybrid composite were larger than nanocomposite, indicating that hybrid composite has a less folding regularity than nanocomposite. © 2008 Wiley Periodicals, Inc. J Appl Polym Sci 108: 870–875, 2008

Key words: crystallization; nanocomposite; biodegradable; cellulose fiber

INTRODUCTION

With a green concept in recent years, the development of biodegradable polymers and their composites (biocomposite) with natural fibers have attracted great interest, both in industry and in academia, because they could allow complete degradation in soil or by composting process and do not emit any toxic or noxious components. These biodegradable polymers are mainly the aliphatic polyesters such as poly(α-hydroxy acid), poly(β-hydroxylalkanoate)s, and poly(ω-hydroxyalkanoate), polyester amides, starch plastics, cellulose derivatives, and soy plastic.[1–6]

Among biocomposites, PLA/natural fiber biocomposites have attracted much attention because PLA can be originally obtained from renewable resources, and natural fibers also have an advantage over conventional fillers. Advanced industrial technologies make it possible to obtain high molecular weight PLA, which leads to a potential for structural materials with enough lifetime to maintain mechanical properties without rapid hydrolysis even under humid environments, as well as good compostability. However, the current price of PLA limits their use to a few exclusive applications such as in the field of bio-medicine. So, now many companies over the world are struggling to accomplish the competitive cost-performance of PLA with conventional polymers, like polyethylene, polypropylene, and polyester. The incorporation of natural fibers will also contribute to a more competitive price.

Furthermore, biodegradable nanocomposites in combination with nano filler reinforcement are expected as the next generation of materials for the future.[7–16] These nanocomposites exhibit remarkable improvements of material properties when compared with the matrix polymers alone or conventional micro- and macro-composite materials. Improvements can include a high strength and stiffness with little sacrifice of toughness, a decrease in gas permeability, and flammability, increased heat distortion temperature, an increase in the biodegradability rate of biodegradable polymers, and so forth.

The authors have actively studied on biodegradable polymer-based biocomposites with natural fibers and cornstarch with designable interfacial properties by chemical modification of both matrix and fillers and by the use of bio-based coupling agents.[17–23] This study focused on the isothermal crystallization behavior of hybrid biocomposite consisting of regenerated cellulose fiber (RCF), organophilic clay, and PLA, comparing pure PLA and PLA/clay nanocomposite.

Correspondence to: S.-H. Lee (lshyhk@hotmail.com).
Contract grant sponsor: National Research Initiative of the USDA Cooperative State Research, Education and Extension Service; contract grant number: 2005-02645.
Contract grant sponsor: USDA Wood Utilization Research Grant.

Journal of Applied Polymer Science, Vol. 108, 870–875 (2008)

The study of the crystallization behavior is of great importance in crystalline polymer/natural fiber composite processing. The control of the temperature profile in the final stage of a process determines the development of a specific morphology which influences the final properties of the composite. In particular, it is known that the crystallinity of matrix in biodegradable biocomposite affects significantly on their biodegradability.

EXPERIMENTAL

Materials

PLA/clay (95/5) nanocomposite (Terramac TE6100) was kindly supplied by Unitika Ltd. (Tokyo, Japan). Lyocell fiber (1.7 decitex), as a regenerated cellulose fiber (RCF), with 10-μm diameter and 38-mm length was kindly supplied from Tencel (NY).

Preparation of hybrid composites

PLA/clay nanocomposite and RCF were first mixed in dry solid states, followed by blending using a batch mixer. The hybrid composite was composed of 70 wt % of nanocomposite and 30 wt % of RCF. Kneading was conducted at 180°C for 15 min with a rotation speed of 50 rpm. The kneaded samples were molded into sheets under 150 kgf/cm^2 pressure at 180°C and then quenched to room temperature.

DSC measurements

DSC measurement was performed on a Perkin–Elmer DSC7 differential scanning calorimeter. The apparatus was calibrated with the indium standard and the samples were placed in sealed aluminum cells. For isothermal crystallization, a hot-pressed sample was first heated to 200°C and maintained at that temperature for 5 min to eliminate its thermal history. Then, it was rapidly cooled to certain isothermal crystallization temperatures (T_{ic}), and crystallized for a certain length of time. After the isothermal crystallization was completely finished, the samples were subsequently cooled to 30°C and then heated again to 200°C at a rate of 10°C/min to estimate melting temperatures.

RESULTS AND DISCUSSION

Isothermal crystallization kinetics

Figure 1 shows the crystallization isotherms of PLA/clay nanocomposite and hybrid PLA/clay/RCF composite by plotting the relative crystallinity against time at the different temperatures. The theory of Avrami was used to analyze the increase of the relative crystallinity ($X(t)$) with time (t) by using the following equation;[24]

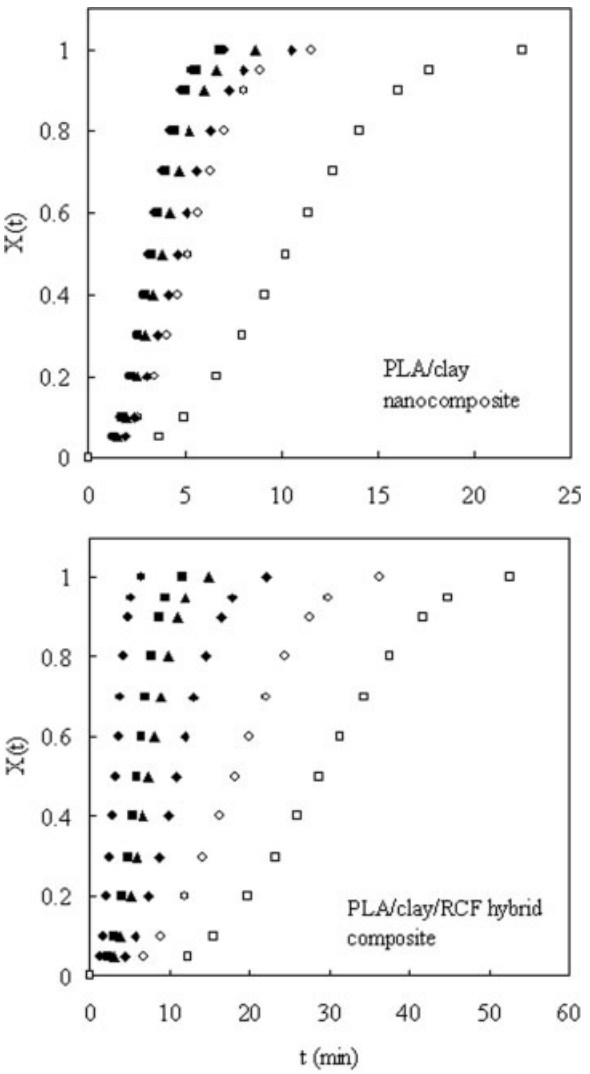

Figure 1 Crystallization isotherms of PLA/clay nanocomposite and PLA/clay/RCF hybrid composite at different temperatures. ●115°C, ■120°C, ▲125°C, ◆130°C, ○135°C, □140°C.

$$1 - X(t) = \exp(-Kt^n) \quad (1)$$

where k is the crystallization rate constant, and n is the Avrami exponent. These values are considered to be diagnostic to the mechanism of crystallization, which are respectively related to the crystallization rate and to the type of nucleation together with the geometry of the crystal growth. Equation (1) can be rewritten as follows;

$$\text{Log}[1 - \text{Ln}\,(1 - X(t))] = \text{Log}\,k + n\text{Log}\,t \quad (2)$$

The Avrami exponent (n) was obtained from the plots of Log[1−Ln(1−$X(t)$)] versus Log t (Fig. 2) and the values are summarized in Table I. Both composites

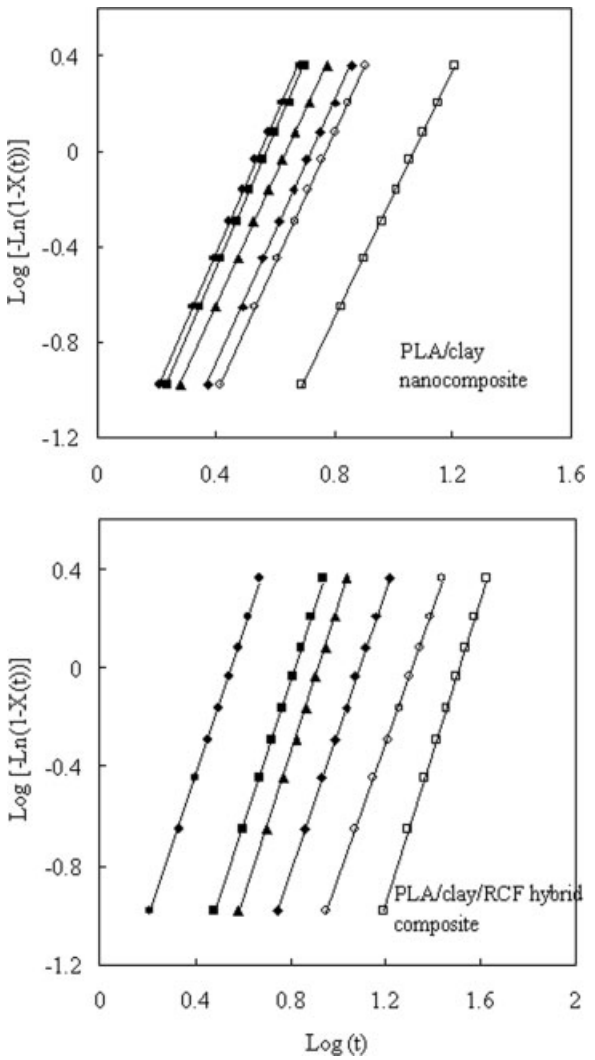

Figure 2 Avrami plots for PLA/clay nanocomposite and PLA/clay/RCF hybrid composite at different temperature. ●115°C, ■120°C, ▲125°C, ◆130°C, ○135°C, □140°C.

showed Avrami exponents of $2.5 < n < 3$. This assumes that there is no limitation on crystal growth direction, because the Avrami exponent of pure PLA is reported around 3 in the same crystallization temperature range.[25] Generally, crystal growth and nucleation are more complicated for the composite, because filler might play the role of nucleation agent or limits normal crystal growth in certain areas.

The crystallization kinetic rate constant (k) is obtained with the following equation;

$$t_{0.5} = (\mathrm{Ln}\ 2/k)^{1/n} \tag{3}$$

where $t_{0.5}$ is the half-crystallization time, which is defined as the time required for half of the final crystallinity to be developed. Figure 3 shows the plot of $t_{0.5}$ versus T_{ic}, indicating that the overall crystallization time of PLA/clay/RCF hybrid composite was longer than PLA/clay nanocomposite in the range of crystallization temperatures explored here. Compared with the crystallization time for PLA at the same temperature range reported by Iannace and Nicolais, both composites showed shorter crystallization time.[25] The values of crystallization rate constant are summarized in Table I. In both composites, the lower the crystallization temperature (T_{ic}), the faster the crystallization. The values of k were higher in PLA/clay nanocomposite than in PLA/clay/RCF hybrid composite at the same crystallization temperature, showing that the addition of RCF into PLA/clay nanocomposite decreased the overall crystallization rate. These values for both composites are higher than those known for the pure PLA.[25]

Equilibrium melting points

The endothermic peak obtained by reheating run after the isothermal crystallization was considered to be the melting temperatures (T_m), corresponding to different crystallization temperature. Figure 4 shows the plot of T_m versus T_{ic} and the line of $T_m = T_{ic}$ was extrapolated. From the crossing point with the line for $T_m = T_{ic}$, the equilibrium melting temperature (T_m^{eq})

TABLE I
Values of Avrami Exponent (n) and the Overall Rate Constant (k) for Isothermal Crystallization

Sample	T_{ic} (°C)	n	k (min^{-n})
PLA/clay nanocomposite	115	2.86	2.69×10^{-2}
	120	2.85	2.35×10^{-2}
	125	2.71	1.87×10^{-2}
	130	2.77	1.01×10^{-2}
	135	2.73	7.81×10^{-3}
	140	2.63	1.53×10^{-3}
PLA/clay/RCF hybrid composite	115	2.91	2.40×10^{-2}
	120	2.94	3.83×10^{-3}
	125	2.94	1.92×10^{-3}
	130	2.88	7.27×10^{-4}
	135	2.74	2.51×10^{-4}
	140	2.97	3.23×10^{-5}

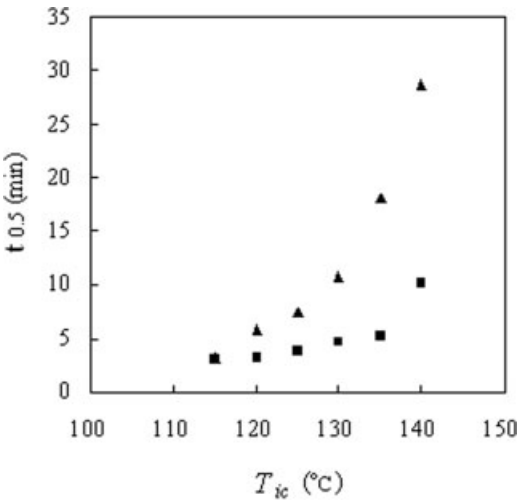

Figure 3 Half-time crystallization as a function of crystallization temperature in PLA/clay nanocomposite (■) and PLA/clay/RCF hybrid composites (▲).

was obtained using the Hoffman–Weeks equation as follows;[26]

$$T_m = \phi T_{ic} - (1 - \phi) T_m^{eq} \quad (4)$$

where ϕ (= $1/\gamma$) is stability parameter, which is usually related to morphological factors concerning perfectness and size of the crystal. The γ is the ratio of the lamellar thickness (l) to the lamellar thickness (l^*) of the critical nucleus at T_{ic}. The value of ϕ can be assumed between 0 and 1. $\phi = 0$ means $T_m = T_m^{eq}$, whereas $\phi = 1$ means $T_m = T_{ic}$, indicating that the crystals are most stable for $\phi = 0$ and are inherently unstable for $\phi = 1$. The values obtained are summarized in Table II. The equilibrium melting temperature

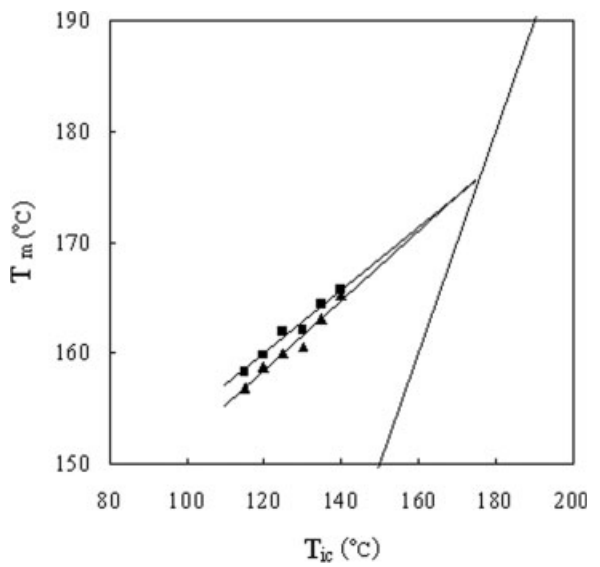

Figure 4 Hoffman–Weeks plots of isothermally crystallized PLA/clay nanocomposite (■) and PLA/clay/RCF hybrid composites (▲).

of hybrid composite was 176.3°C, which is almost same with that of nanocomposite. These values are lower than those for PLA reported in the literature.[27–30,31] Marand et al. reported that the value of PLLA is around 225°C by using the equation to eliminate the effect of the isothermal thickening process on experimentally observed melting temperature.[31] Iannace and Nicolais reported 206°C for PLLA.[25] Teramoto et al. and Nam et al. also reported 177 and 179°C, respectively, for PLLA. The stability parameters in both samples were less than 0.4, suggesting that the crystals are fairly stable. The value of φ of the hybrid composite was larger than that of nanocomposite, indicating that the hybrid composite formed a more unstable crystal.

Crystallization activation energy

Activation energy for crystallization can be obtained from the relationship between crystallization rate constant (k) and T_{ic} by the following Arrhenius form;[32]

$$K^{1/n} = K_0 - \exp\left(-\Delta E / R T_{ic}\right) \quad (5)$$

$$\frac{1}{n} \mathrm{Ln}\, K = \mathrm{Ln}\, K_0 - \frac{\Delta E}{R T_{ic}} \quad (6)$$

where K_0 is a constant related to the initial crystallization rate, R is the absolute gas constant, and ΔE is the activation energy of crystallization. The ΔE is determined as the slope coefficient by plotting $\frac{1}{n}\mathrm{Ln}\, K$ against $\frac{1}{T_{ic}}$ as shown in Figure 5. The values of ΔE for nanocomposite and hybrid composite were found to be -57.52 and -108.06 kJ/mol, respectively. The obtained values were negative, which is due to the energy released during transforming the molten state into the crystalline state. Activation energy of hybrid composite was larger than that of nanocomposite, which means that the crystallization rate of hybrid composite was more temperature dependent. Furthermore, the difference between crystallization rate constants of hybrid composite and nanocomposite became higher at higher crystallization temperature, showing that hybrid composite accelerates the crystallization of PLA at lower crystallization temperature.

TABLE II
Equilibrium Melting Temperature (T_m^{eq}), Stability Parameter (ϕ), Nucleation Parameter (K_g), and the Surface Free Energy (σ_e)

Sample	T_m^{eq}	ϕ	K_g (10^3 K^2)	σ_e (10^{-5} J/cm^2)
PLA/clay nanocomposite	176.0	0.29	200	0.47
PLA/clay/RCF hybrid composite	176.3	0.32	243	0.58

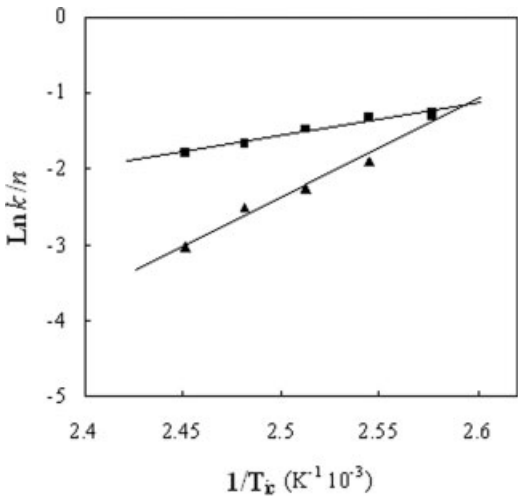

Figure 5 Plot of Ln k / n versus $1/T_{ic}$. PLA/clay nanocomposite (■), PLA/clay/RCF hybrid composites (▲).

Analysis of kinetic data according to nucleation theories

The overall rate constant (k) or the half-time of crystallization ($t_{0.5}$) is closely related to crystallization rate G as follows;[33,34]

$$G \propto t_{0.5}^{-1} = \frac{K^{1/n}}{\text{Ln } 2^{1/n}} \tag{7}$$

According to kinetic theory developed by Hoffman et al., the dependency of crystal growth rate, G on the crystallization temperature T_{ic} is expressed by the following equation;[35,36]

$$G = G_0 \exp\left(\frac{-U^*}{R(T_{ic} - T_\infty)}\right) \exp\left(\frac{-K_g}{T_{ic}(\Delta T)f}\right) \tag{8}$$

where G_0 is a preexponential factor generally assumed to be constant or proportional to T_{ic}, U^* is an activation energy for segmental diffusion to the site of crystallization, R is the absolute gas constant, and T_∞ is the hypothetical temperature below which all viscous flow ceases, K_g is the nucleation parameter, ΔT is the degree of supercooling defined by $T_m^{eq} - T_{ic}$. The correction term f ($= 2T_{ic}/T_{ic} + T_m^{eq}$) is introduced to account for change in heat of fusion with the crystallization temperature. It is important to emphasize that the parameters U^* and T_∞ are treated as variables to maximize the quality of the fit to eq. (8). U^* can be calculated with the Williams–Landel–Ferry (WLF) relation as follows;[33]

$$U^* = \frac{C_1 T_c}{C_2 + T_c - T_g} \tag{9}$$

where C_1 and C_2 are constants (generally assumed to be 4120 cal/mol and 51.6 K). T_∞ ($T_g - 51.6$) is also used. K_g is given by

$$K_g = \frac{Y b_0 \sigma \sigma_e T_m^{eq}}{k_B \Delta H_u} \tag{10}$$

where ΔH_u is the heat of fusion of completely crystalline component (174×10^6 J/m^3) was adopted in this work), Y is a coefficient that depends on the regime of crystal growth, σ and σ_e are the lateral surface energy and the fold surface free energy, respectively, and b_0 is the layer thickness, k_B is Boltzmanns constant. Generally, the Y value is 4, when T_{ic} values lie in regime I (lower ΔT) and III (higher ΔT), and is 2 for the regime II growth process (medium ΔT). In this study, it is assumed that the growth front is the (110) plane as the same with PLA ($b_0 = 0.53$ nm) and mode of spherulite growth is regime II growth.

Figure 6 shows the plot of the Ln $(1/t_{0.5}) + U^*/R(T_{ic} - T_g)$ and $1/(fT_{ic}\Delta T)$ and the value of K_g, calculated from the slopes, are listed in Table II. It was found that the K_g value of hybrid composite was larger than that of nanocomposite. This value represents the free energy necessary to form a nucleus of critical size, so it can be said that hybrid composites needs less energy to form the nucleus of critical size than nanocomposite.

The derived K_g values can be used to calculate the surface free energy (σ_e). The lateral surface free energy (σ) of linear polymer crystals can be estimated with following relation holds.

$$\sigma = (0.23) b_0 \Delta H_u \tag{11}$$

The values obtained are also summarized in Table II. The surface free energy of hybrid composite was larger than that of nanocomposite. The increase of surface free energy in hybrid composite indicates that the combination of clay and RCF provides a less

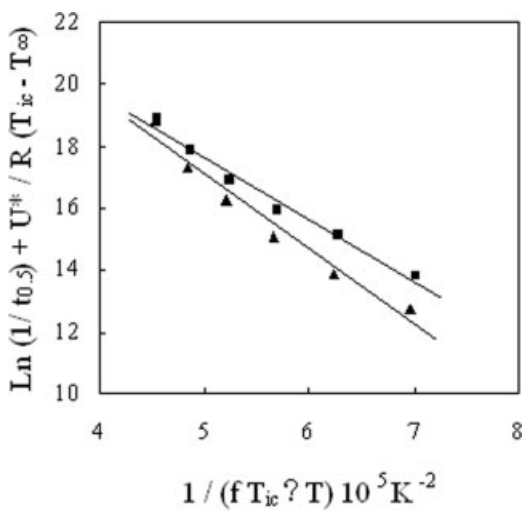

Figure 6 Plot of the Ln $(1/t_{0.5})$ + U*/R$(T_{ic} - T_\infty)$ and $1/(fT_{ic}\Delta T)$. PLA/clay nanocomposite (■), PLA/clay/RCF hybrid composites (▲).

folding regularity on lamellar surfaces. Compared with the σ_e value of 0.41×10^5 and 0.34×10^5 (J cm^{-2}) for PLLA reported by Di Lorenzo and Teramoto et al., respectively, the values for both composites were higher, showing that the filler increased the folding irregularity in the process of crystallization.[27,37]

CONCLUSION

Generally, the crystallization behavior is of importance in determining of a specific morphology of the composite, which affects the final properties. In this study, how the isothermal crystallization behavior of PLA/clay nanocomposite is affected by regenerated cellulose fiber (RCF) was investigated by DSC measurement. As a conclusion, RCF delayed the overall crystallization rate of nanocomposite and decreased the value of crystal stability parameter. Activation energy of hybrid composite was larger than that of nanocomposite, indicating that the crystallization rate of hybrid composite was more temperature dependent. The increase surface free energy (σ_e) for folded lamellar crystals of PLA in hybrid composite indicated that the addition of RCF to nanocomposite increases the irregularity of folding surface.

References

1. Mohanty, A. K.; Misra, M.; Hinrichsen, G. Macromol Mater Eng 2000, 276/277, 1.
2. Shibata, M.; Oyamada, S.; Kobayashi, S.; Yaginuma, D. J Appl Polym Sci 2004, 92, 3857.
3. Nishino, T.; Hirao, K.; Kotera, K.; Nakamae, K.; Inagaki, H. Composite Sci Technol 2003, 63, 1281.
4. Rosa, D. S.; Rodrigues, T.; Guedes, C. G.; Calil, M. R. J Appl Polym Sci 2003, 89, 3539.
5. Shogren, R. L.; Doane, W. M.; Garlotta, D.; Lawton, J. W.; Willett, J. L. Polym Degrad Stabil 2003, 79, 405.
6. Wu, C. S. J Appl Polym Sci 2003, 89, 2888.
7. Ray, S. S.; Okamoto, M. Progress Polym Sci 2003, 28, 1539.
8. Schmidt, D.; Shah, D.; Giannelis, E. P. Curr Opin Solid State Mater Sci 2002, 6, 205.
9. Someya, Y.; Nakazato, T.; Teramoto, N.; Shibata, M. J Appl Polym Sci 2004, 91, 1463.
10. Messersmith, P. B.; Giannelist, E. P. J Polym Sci Part A: Polym Chem 1995, 33, 1047.
11. Ogata, N.; Kawakage, S.; Ogihara, T. J Appl Polym Sci 1997, 66, 573.
12. Lim, S. T.; Hyun, Y. H.; Choi, H. J.; Jhon, M. S. Chem Mater 2002, 14, 1839.
13. Aranda, P.; Hitzky, E. R. Chem Mater 1992, 4, 1395.
14. Ray, S. S.; Yamada, K.; Ogami, A.; Okamoto, M.; Ueda, K. Macromol Rapid Commun 2002, 23, 943.
15. Hiroi, R.; Ray, S. S.; Okamoto, M.; Shiroi, T. Macromol Rapid Commun 2004, 25, 1359.
16. Maiti, P.; Yamada, K.; Okamoto, M.; Ueda, K.; Okamoto, K. Chem Mater 2002, 14, 4654.
17. Lee, S. H.; Wang, S. Compos A: Appl Sci Manufact 2006, 37, 80.
18. Ohkita, T.; Lee, S. H. J Appl Polym Sci 2005, 97, 107.
19. Ohkita, T.; Lee, S. H. J Appl Polym Sci 2006, 100, 3009.
20. Lee, S. H.; Ohkita, T.; Kitagawa, K. Holzforschung 2004, 58, 529.
21. Lee, S. H.; Ohkita, T. Holzforschung 2004, 58, 537.
22. Ohkita, T.; Lee, S. H. J Adhesion Sci Technol 2004, 18, 905.
23. Lee, S. H.; Ohkita, T. J Appl Polym Sci 2003, 90, 1900.
24. Avrami, M. Chem J Phys 1940, 8, 212.
25. Iannace, S.; Nicolais, L. J Appl Polym Sci 1997, 64, 911.
26. Hoffman, J. D.; Weeks, J. J Chem Phys 1962, 37, 1723.
27. Teramoto, Y.; Nishio, Y. Biomacromolecules 2004, 5, 397.
28. Nam, J. Y.; Ray, S. S.; Okamoto, M. Macromolecules 2003, 36, 7126.
29. Abe, H.; Kikkawa, Y.; Inoue, Y.; Doi, Y. Biomacromolecules 2001, 2, 1007.
30. Vasanthakumari, A.; Pennings, J. Polymer 1983, 24, 175.
31. Marand, H.; Xu, J.; Srinivas, S. Macromolecules 1998, 31, 8219.
32. Cebe, P.; Hong, S. D. Polymer 1986, 27, 1183.
33. Allen, R. C.; Madelkern, L. Polym Bull 1987, 17, 473.
34. Nishio, Y.; Hirose, N.; Takahashi, T. Sen'I Gakkaishi 1990, 46, 441.
35. Hoffman, J. D.; Davis, G. T.; Lauritzen, J. I. Treatise on Solid State Chemistry: Crystalline and Non-crystalline Solid; Plenum: New York, 1976.
36. Hoffman, J. D.; Frolen, L. J.; Ross, G. S.; Lauritzen, J. I. J Res Natl Bureau Standards A: Phys Chem 1975, 79A, 671.
37. Di Lorenzo, M. L. Polymer 2001, 42, 9441.